Improved Mindlin Plate Stress Analysis for Laminated Composites in Finite Element Method

Maenghyo Cho* and Jun-Sik Kim†
Inha University, Inchon 402-751, Republic of Korea

I. Introduction

DUE to their light weight and high stiffness, advanced laminated composites are used as primary structural components in aircraft, and many research papers have focused on the analysis of laminated composite plates. As a practical analysis and design tool, finite elements have been developed based on numerous plate theories. They include smeared higher-order theories, layerwise theories, and simplified zigzag higher-order theories. An excellent review for this research field can be found in Ref. 1. The finite elements based on polynomial-based theories cannot predict accurately transverse shear stresses because they satisfy neither top and bottom stress-free conditions nor interface stress continuity conditions. Finite elements based on layerwise theories provide accurate stresses through the thickness.[2] However, they require layer-dependent degrees of freedom. Thus, they are not efficient at analyzing thick laminates. An efficient higher-order plate theory (EHOPT) developed by Cho and Parmerter[3] belongs to simplified zigzag higher-order theories. This provides accurate global and through-the-thickness plate behavior. However, when implemented in a finite element, it requires a C_1 condition between elements and a large amount of computations are needed to calculate the element stiffness matrix.

Thus, a method to predict stress accurately without solving the complicated equilibrium equations of EHOPT has been pursued by Cho and Kim.[4] They match the primary variables of both EHOPT and first-order shear deformation plate theory (FOPT) by assuming the transverse shear strain energies of both theories to be equivalent. After obtaining FOPT solutions, the matched EHOPT in-plane displacement field can be used as a postprocessor to improve the FOPT stresses and deformations. The validity of this postprocess method was demonstrated in Ref. 4.

A numerical stress recovery technique that works in a finite element framework has been developed. It has shown that a postprocess method using an orthogonal polynomial can be used in the finite element method (FEM).[5] The method using orthogonal polynomials is efficient in obtaining higher-order derivatives. However, it is not easy to apply this method to various plate geometric configurations. To overcome this difficulty, the present study proposes a numerical postprocess method that can obtain higher-order derivatives at the element level instead of at the global level.

The validity of the present method is demonstrated by comparing its numerical solution to analytical solutions of the postprocess method.

II. Postprocess Method

The displacement fields of an FOPT and an EHOPT as a postprocessor are as follows:

$$u_\alpha = u^o_\alpha(x_1, x_2) + z\,\psi_\alpha(x_1, x_2) \qquad u_3 = w(x_1, x_2) \tag{1}$$

$$u_\alpha = u^o_\alpha + \psi_\alpha z - \frac{4z^3}{3h^2}\left[w_{,\alpha} + \psi_\alpha + \sum_{k=1}^{N/2-1} a^k_{\alpha\gamma}(\psi_\gamma + w_{,\gamma}) \right]$$
$$+ \sum_{k=1}^{N/2-1} a^k_{\alpha\gamma}(\psi_\gamma + w_{,\gamma})[(z - z_k)H(z - z_k) \tag{2}$$
$$-(z - z_k)H(z - z_k)]$$
$$u_3 = w(x_1, x_2) \text{(subscript } \alpha \text{ can be of value 1 or 2)}$$

where N is the number of layers, $H(z - z_k)$ is the Heaviside unit step function, and $a^k_{\alpha\gamma}$ can be determined from layer transverse material properties and layer thickness. A detailed derivation of Eq. (2) can be found in Ref. 3.

Matching the Rotational Variables

The variables of the EHOPT can be obtained in terms of the variables of FOPT by assuming the transverse shear energy of EHOPT and FOPT to be equivalent:

$$U^{\text{EHOPT}}_{\text{shear}} = U^{\text{FOPT}}_{\text{shear}} \tag{3}$$

where U_{shear} denotes the transverse shear strain energy of the laminated composites.

This relationship can be expressed as

$$(\psi_\alpha + w_{,\alpha})^{(\text{EHOPT})} = C_\alpha(\psi_\alpha + w_{,\alpha})^{(\text{FOPT})} \tag{4}$$

with no summation in α. C_α is the matching factor. It is assumed that the out-of-plane deflection w of EHOPT is the same as that of FOPT. A derivation of Eqs. (3) and (4) can be found in Ref. 3.

Shear Correction Factor

To improve the global response of the FOPT, shear correction factors are introduced in the FOPT. In the present study, two ways of calculating shear correction factors are used: 1) the iterative calculation method[6] and 2) the direct calculation method.[7]

In general, the first method is more accurate than the second because the shear correction factor depends on the loading condition, boundary condition, geometry, and layup configurations. However, from the FEM perspective, the second method is better than the first method. In the present Note, both methods are applied and the results are compared.

The postprocess method flowchart is given in Fig. 1.

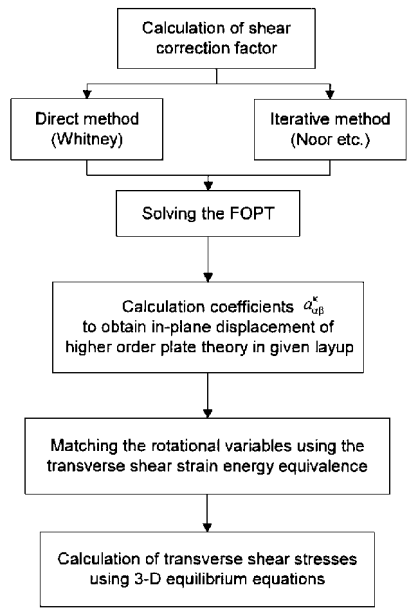

Fig. 1 Flowchart of a postprocess method.

Received Aug. 11, 1995; revision received July 25, 1996; accepted for publication Nov. 21, 1996; also published in *AIAA Journal on Disc*, Volume 2, Number 2.

*Assistant Professor, Department of Aerospace Engineering, 253 Yong-Hyun Dong, Nam-ku. Member AIAA.

†Graduate Research Assistant, Department of Aerospace Engineering, 253 Yong-Hyun Dong, Nam-ku.

III. Finite Element Formulation

To formulate a finite element of first-order shear deformation plate theory, each dependent variable is expressed in terms of shape functions and nodal unknowns:

$$u_\alpha^o = \sum_{i}^{N} N_i u_{\alpha i}^o, \qquad \psi_\alpha = \sum_{i}^{n} N_i \psi_{\alpha i}, \qquad w = \sum_{i}^{n} N_i w_i \quad (5)$$

where n is the number of node points of an element and N_i is a shape function for the ith node.

The transverse shear stress of the postprocess phase is calculated accurately by integrating equilibrium equations through the thickness. Higher-order derivatives of out-of-plane deflection w need to be calculated to obtain accurate transverse shear stresses by integrating equilibrium equations. This makes FEM implementation of the postprocess method difficult. Therefore, the following methods are proposed for numerical calculation of higher-order derivatives: 1) interpolation method, a) local interpolation[8] and b) global interpolation[5]; 2) direct application of higher-order element (12-noded element, etc.); 3) application of Green theorem to equilibrium equations[9]; and 4) using the difference of second derivatives between elements.

Method 1a transforms an 8-noded element into a 12-noded element by the least-squares fitting of nodal values over the elements.[8] Transverse shear stresses can be calculated within an element but the calculation process is complicated. Method 1b interpolates the nodal values over the global domain by using orthogonal polynomials.[5] Although accurate, it is difficult to apply this method to various geometries. Method 2 is direct and simple because it generates third derivatives inside of an element with the element shape functions. However, a higher-order element is needed for this calculation. In the present study, a 12-noded element is used for this direct calculation of third derivatives. Method 3 was used in Ref. 9. Divergence theorem was applied to the three-dimensional stress equilibrium equations at the element level to utilize only the lower-order derivatives. It is efficient if second derivatives do not appear in the in-plane stress expressions. Method 4 can provide an accurate prediction of third derivatives of w with a relatively small number of nodal values if a nine-noded element, which generates constant second-order derivatives within an element, is used.

In the present Note, results of method 1b will be shown because method 1a has basically the same features. To apply methods 2 and 4, a Serendipity 12-noded element and a Lagrangian 9-noded element are used.

IV. Numerical Examples and Results

Numerical solutions for symmetric cross-ply are evaluated to assess the accuracy of the present postprocess method. The three-dimensional elasticity solutions of Pagano[10] for simply supported rectangular plates under sinusoidal loading are reproduced here for comparison. Two examples are considered: case 1, a three-layer square laminate [0/90/0] with uniform ply thickness; and case 2, a nine-layer square laminate [0/90/ ... /90/0].

Both plates are under sinusoidal loading conditions. The material properties for the 0-deg layer are

$$E_1 = 25 \times 10^6 \text{ psi}, \quad E_2 = 10^6 \text{ psi}, \quad G_{12} = G_{13} = 0.5 \times 10^6 \text{ psi}$$
$$G_{23} = 0.2 \times 10^6 \text{ psi}, \quad v_{12} = v_{13} = v_{23} = 0.25$$

To facilitate the comparison with other theories, the following nondimensional parameters are defined:

$$(\bar{\sigma}_{xx}, \bar{\sigma}_{yy}, \bar{\sigma}_{xy}) = \frac{h^2}{q_o a^2}(\sigma_{xx}, \sigma_{yy}, \sigma_{xy})$$

$$(\bar{\sigma}_{yz}, \bar{\sigma}_{xz}) = \frac{h}{q_o a}(\sigma_{yz}, \sigma_{xz}) \quad (6)$$

$$(\bar{u}, \bar{v}) = \frac{E_2 h^2}{q_o a^3}(u, v), \qquad \bar{w} = \frac{100 E_2 h^3}{q_o a^4} w$$

Taking advantage of the symmetry of loading, boundary conditions, and lamination configurations, only quadrants of square plates are used in the finite element analysis. In Table 3 and Figs. 3 and 4, PT(AL), PT(FE9), and PT(FE12) denote analytical postprocess solutions, FEM solutions with a 9-noded element (6×6 mesh), and FEM solutions with a 12-noded element (4×4 mesh), respectively.

Shear Correction Factor

Shear correction factors (SCFs) are introduced to improve the global response of a first-order shear deformation theory solution. In cross-ply cases, shear correction factors are calculated in Table 1. In this study, SCFs are calculated in two ways: the first is Whitney's[7] direct method and the second is the iterative one of Noor and Burton.[6] Two methods generate a 7% difference in SCF k_1^2, as shown in Table 1. Both methods provide accurate transverse deflections.

Calculation of Third Derivatives

The third-derivative calculations are listed in Table 2, and their application is limited to higher-order elements. For the square plate, as shown in Fig. 2, regular and distorted meshes are used for derivative calculations. Compared to analytical solutions, the numerical derivatives in the square plate were calculated within a maximum error of 3.4% at given points in regular meshes and 4.5% error in distorted meshes. Thus, regular mesh provides very accurate third derivatives and, even in distorted mesh, third derivatives can be obtained with reasonable accuracy.

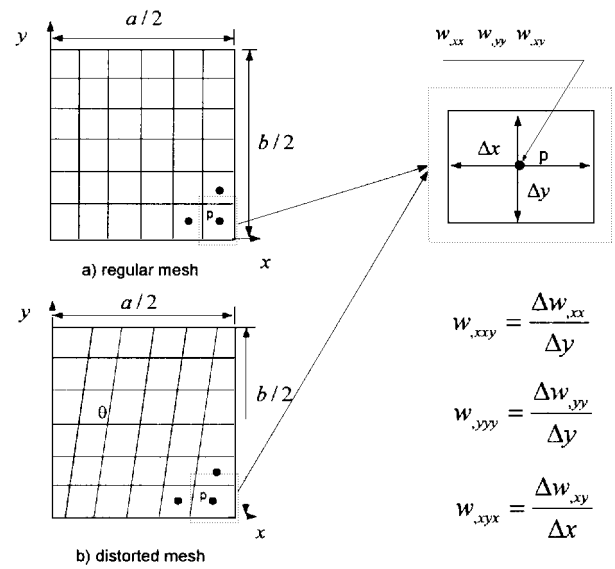

Fig. 2 Mesh configurations of third derivative's comparison.

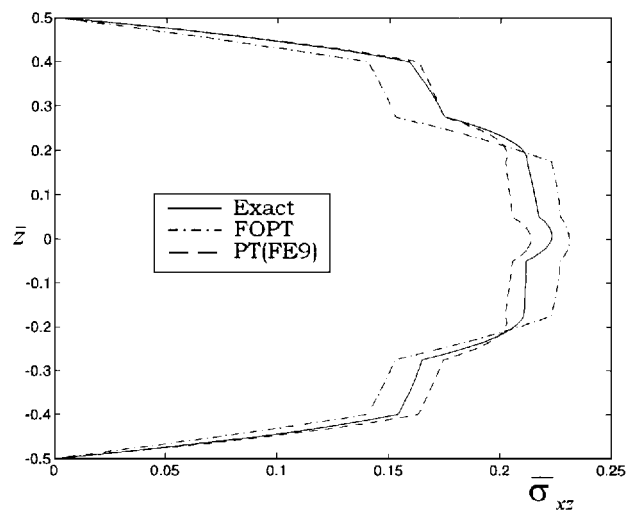

Fig. 3 Transverse shear stresses with nine-noded element of a nine-layered square plate ($S = 4$).

Table 1 Comparison of shear correction factor

	Three-layered plate			Nine-layered plate		
SCF	Whitney[7]	Noor[6]	Noor (FEM)[6]	Whitney[7]	Noor[6]	Noor (FEM)[6]
k_1^2	0.58278	0.57992	0.57946	0.68913	0.67742	0.68506
k_2^2	0.80278	0.86500	0.85627	0.61123	0.62156	0.61997
$\bar{w}$[a]	2.21597	2.20547	2.20881	1.82884	1.82212	1.82483

[a] $\bar{w} = 2.00591$ (three-layered plate), 1.75897 (nine-layered plate).

Table 2 Comparison of third derivatives for [0/90/0] square laminated plate with $a = 4$, $h = 1$, and $k_1 = k_2 = \frac{5}{6}$

	$b = a$			
	Regular mesh	Distorted mesh ($\theta = 11.8$ deg)	Analytical	Analytical
p[a]	(1.83333, 0.16667)	(1.76388, 0.16667)	(1.83333, 0.16667)	(1.76388, 0.16667)
$w_{,yyy}$	2.10661×10^{-6}	2.22195×10^{-6}	2.16485×10^{-6}	2.14610×10^{-6}
$w_{,xxy}$	2.10449×10^{-6}	2.10051×10^{-6}	2.16485×10^{-6}	2.14610×10^{-6}
$w_{,xyx}$	2.09112×10^{-6}	2.10661×10^{-6}	2.16485×10^{-6}	2.14610×10^{-6}

[a] Maximum value p(2, 0): $w_{,yyy} = w_{,xxy} = w_{,xyx} = 2.20238 \times 10^{-6}$.

Table 3 Maximum stresses of [0/90/0] three-layered square plate [$S = a/h$) = 4]

Source[a]	$\bar{\sigma}_x$	$\bar{\sigma}_y$	$\bar{\sigma}_{xz}$	$\bar{\sigma}_{yz}$	$\bar{\sigma}_{xy}$
Exact[10]	0.8010	0.5340	0.2560	0.2172	−0.0511
	−0.7550	−0.5560			0.0505
EHOPT[11]	−0.8175	0.6032			−0.0500
PT(AL)	−0.8976	0.6630	0.2236	0.2530	−0.0554
PT(FE12)	−0.9525	0.6809	0.2921	0.2454	−0.0572
PT(FE9)	−0.8839	0.6510	0.2263	0.2476	−0.0543
FOPT	−0.4370	0.4774	0.1968	0.3368	−0.0369
CPT[10]	−0.5390	0.1800	0.3950	0.0823	−0.0213

[a] CPT, classic plate theory.

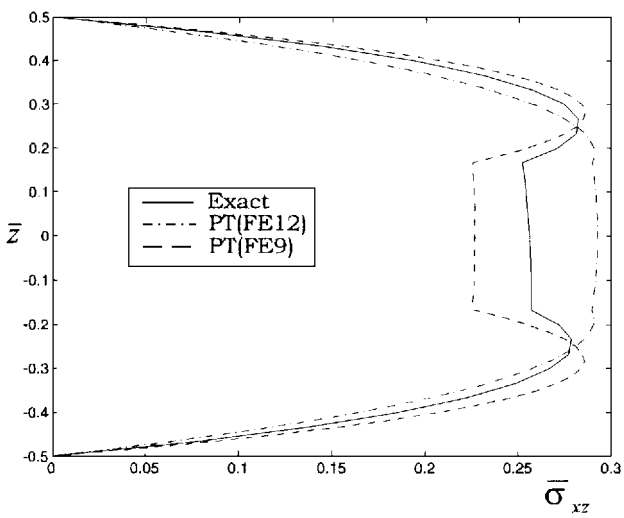

Fig. 4 Comparison of transverse shear stresses with 9-noded element and 12-noded element of a three-layered square plate ($S = 4$).

In-Plane Stresses and Transverse Shear Stresses

The analysis results of case 1 are given in Table 3. The accuracy of transverse shear stresses as well as in-plane stresses are good. The present method is compared to the EHOPT FEM solution[11] for the thick case ($a/h = 4$). The in-plane stresses of the latter are better than those of the former as expected, but the difference between them is very small. Thus, the present postprocess method provides stresses with an accuracy comparable to the original EHOPT solutions. Figure 3 shows the transverse shear stresses of a nine-layered problem. There is good agreement between the proposed postprocess method and the exact elasticity method. In addition, the interlaminar shear stress agrees very well with that of exact elasticity.

Comparison of Performance for the 12-Noded Element and the 9-Noded Element

Figure 4 shows the transverse shear stresses of the 12-noded element and the 9-noded element compared to those of elasticity solutions. The 12-noded element does not predict the shape of exact elasticity solutions because of the inaccuracy of its third derivatives. On the other hand, the nine-noded element can generate accurate second derivatives in each element. Thus, the computed third derivatives using the difference of this second derivative between adjacent elements is more accurate than those from the 12-noded element obtained by direct calculation of the third derivative. Thus, the 9-noded Lagrange element with a higher derivative calculation method provides a better stress prediction than a 12-noded element when compared on the basis of the same number of nodes.

V. Conclusion

This study showed that the accuracy of in-plane and transverse stresses can be improved through the thickness of the plates by applying a postprocessing method analytically and numerically. Although finite elements based on complicated higher-order theories or layerwise theories provide fairly accurate stresses, they are numerically intensive. In this Note, calculation methods to obtain higher-order derivatives are proposed to apply the postprocess method to isoparametric finite elements. Among them, the method that utilizes the difference of second derivatives in the nine-noded element was shown to be convenient and accurate for predicting transverse shear stresses.

Two calculation methods of shear correction factor are used. The analytical and numerical solutions using the present postprocess method demonstrate that both calculation methods of shear correction factors work well in the postprocess routine.

The present postprocess method is limited to symmetric lamination. To apply the method to various configurations, it is necessary to develop a general postprocess method, which is now in progress.

References

[1] Noor, A. K., and Burton, W. S., "Assessment of Shear Deformation Theories for Multilayered Composite Plates," *Applied Mechanics Review,* Vol. 42, No. 1, 1989, pp. 1–13.

[2] Reddy, J. N., and Barbero, E. J., "A Plate Bending Element Based on a Generalized Laminated Plate Theory," *International Journal for Numerical Methods in Engineering,* Vol. 28, No. 10, 1989, pp. 2275–2292.

[3]Cho, M., and Parmerter, R. R., "An Efficient Higher Order Plate Theory for Laminated Composites," *Composite Structures*, Vol. 20, 1992, pp. 113–123.

[4]Cho, M., and Kim, J. H., "Postprocess Method Using a Displacement Field of Higher-Order Laminated Composite Plate Theory," *AIAA Journal*, Vol. 34, No. 2, 1996, pp. 362–368.

[5]Byun, C., and Kapania, R. K., "Prediction of Interlaminar Stresses in Laminated Plates Using Global Orthogonal Interpolation Polynomials," *AIAA Journal,* Vol. 30, No. 11, 1992, pp. 2740–2749.

[6]Noor, A. K., and Burton, W. S., "Stress and Free Vibration Analysis of Multilayered Composite Plates," *Composite Structures*, Vol. 11, 1989, pp. 183–204.

[7]Whitney, J. M., "Shear Correction Factors for Orthotropic Laminates Under Static Load," *Journal of Applied Mechanics*, Vol. 40, March 1973, pp. 302–304.

[8]Kouri, J. V., and Atluri, S. N., "Analytical Modelling of Laminated Composites," *ICCMSAMPE*, edited by S. W. Tsai and G. S. Springer, Vol. 8, 1992, pp. 30A1–30A15.

[9]Chaudhuri, R. A., "An Equilibrium Method for Prediction of Transverse Shear Stresses in a Thick Laminated Plate," *Computers and Structures*, Vol. 23, No. 2, 1986, pp. 139–146.

[10]Pagano, N. J., "Exact Solutions for Rectangular Bidirectional Composites and Sandwich Plates," *Journal of Composite Materials*, Vol. 4, No. 1, 1970, pp. 20–34.

[11]Cho, M., and Parmerter, R. R., "Finite Element for Composite Plate Bending Based on Efficient Higher Order Theory," *AIAA Journal*, Vol. 32, No. 11, 1994, pp. 2241–2248.

R. K. Kapania
Associate Editor

Free-Vibration Analysis of Turbine Blades Using Nonlinear Finite Element Method

D. Dhar* and A. M. Sharan†
Memorial University of Newfoundland, St. John's, Newfoundland A1B 3X5, Canada

Nomenclature

c	= specific heat
$[CP]$	= capacitance matrix
e	= element
$\{F_c\}$	= force vector due to convection
$\{F_r\}$	= force vector due to radiation
G	= global
h	= convective heat transfer coefficient
$[K_s]$	= conventional stiffness matrix
$[K_\sigma]$	= stress stiffness matrix
$[KC]$	= conduction matrix
k_x, k_y, k_z	= thermal conductivities in the x, y, and z directions, respectively
l_x, l_y, l_z	= direction cosines normal to the surface
$[M]$	= mass matrix
Q	= heat generated within the body
q	= specified heat flux
$\{T\}$	= nodal temperature vector
T_∞	= gas temperature
t	= time
ϵ	= emissivity of the body
λ	= eigenvalue of the system
σ	= Stefan–Boltzmann constant

Received Feb. 4, 1995; revision received May 17, 1996; accepted for publication Dec. 26, 1996; also published in *AIAA Journal on Disc*, Volume 2, Number 2.

*Graduate Student, Faculty of Engineering and Applied Sciences.

†Professor, Faculty of Engineering and Applied Sciences.

I. Introduction

BEFORE designing a turbine blade, it is essential to know its undamped natural frequencies, and there are various reasons for it. Right from the start until it comes to a constant operating speed, the rotor goes through the various blade natural frequencies. To avoid resonance, the steady-state operating speed should not match the system natural frequencies. As the temperature of the turbine blade changes with time, there is a change in the material properties of the turbine blade. This change in the material property of the turbine blade is reflected in the change in the conventional stiffness matrix $[K_s]$ of the blade, and this causes a change in the natural frequencies of the turbine blade. There is also a significant change in the natural frequencies because of the variational effect of the stress stiffness matrix $[K_\sigma]$, which is nonlinear in nature and is caused by higher deflections during the rotation of the turbine blade.

Sato[1] used the Ritz method to study the effect of axial force on the frequencies of blades with ends restrained elastically against rotation. Sisto and Chang[2] formulated a finite element model to calculate the natural frequencies of the blade. Their model, however, was appropriate for thin and high-aspect-ratio blades only. Sharan and Bahree[3] did the transient-free-vibration analysis of the turbine blade using 20-noded finite elements, which included the effect of the two-dimensional change in temperature. The effect of the stress stiffness matrix, caused by the rotation of the turbine blade, was not included in their study. Warikoo[4] analyzed the propeller-shafttransverse vibrations. His work included the nonlinear stiffness variation but did not include the effect of change in the temperature on the transient natural frequencies of the turbine blade. Dhar[5] carried out extensive studies of the three-dimensional heat transfer process in the turbine blades. He found that there was significant temperature gradient along the height of the blade that was not accounted for in the earlier two-dimensional studies.

In the present investigation, the authors study the combined effects of three types of nonlinearities (the radiative heat flux, the nonlinear stiffness matix, and the material property variation due to the change in the temperature) on the natural frequencies of the turbine blade. Instead of Sharan and Bahree's two-dimensional heat transfer model,[3] a three-dimensional heat transfer model has been used in the present work.

II. Mathematical Formulation

To obtain the blade frequencies as a function of time, one has to solve the eigenvalue problem, which can be stated as

$$[K^G]\{x\} - \lambda[M^G]\{\ddot{x}\} = 0 \tag{1}$$

where $[K^G]$ is obtained by adding $[K_s^G]$ and $[K_\sigma^G]$. Along with this, one also has to solve for the transient temperatures, which change the elastic properties of the material. The three-dimensional nonlinear heat transfer equation is given by

$$k_x\frac{\partial^2 T}{\partial x^2} + k_y\frac{\partial^2 T}{\partial x^2} + k_z\frac{\partial^2 T}{\partial z^2} + Q = \rho c\frac{\partial T}{\partial t} \tag{2}$$

and its nonlinear boundary condition as

$$k_x\frac{\partial T}{\partial x}l_x + k_y\frac{\partial T}{\partial y}l_y + k_z\frac{\partial T}{\partial z}l_z + h(T - T_\infty) + q + \sigma\epsilon(T^4 - T_\infty^4) = 0 \tag{3}$$

The mathematical details of obtaining the global equations using the finite element analysis for Eqs. (1) and (3) are given elsewhere.[5] The global equation for Eq. (3) can be written as

$$[CP^G]\frac{\partial\{T^G\}}{\partial t} + [KC^G]\{T^G\} = \{F_c^G\} + \{F_r^G\} \tag{4}$$

At first, one solves for the temperatures at a given instant of time, and then the material properties are evaluated to obtain the frequencies by solving for the eigenvalues as stated in Eq. (1).